International Food Research Journal 28(3): 423 - 434 (June 2021)

Journal homepage: *http://www.ifrj.upm.edu.my*

Effect of feeding type and artisanal process in microstructural and physicochemical parameters of fresh and ripened goat cheese

[1,2]Ramírez-Rivera, E. J., [3]Herrera-Corredor, J. A., [4]Toledo-López, V. M., [4]Sauri-Duch, E., [5]Rodriguez-Miranda, J., [6]Juárez-Barrientos, J. M., [7]Díaz-Rivera, P. and [5]*Herman-Lara, E.

[1]*Tecnológico Nacional de México / Instituto Tecnológico Superior de Zongolica, Km 4 Carretera Tepetitlanapa, 95005 Zongolica, Veracruz, México*

[2]*Centro de Investigación y Asistencia en Tecnología y Diseño del Estado de Jalisco A.C. Sede Sureste, Tablaje Catastral 31264 Km. 5.5 Carretera Sierra Papacal-Chuburna Puerto Parque Científico Tecnológico de Yucatán, 97302 Mérida, Yucatán, México*

[3]*Colegio de Postgraduados Campus Córdoba, Km. 348 Carretera Federal Córdoba-Veracruz, 94500 Córdoba, Veracruz, México*

[4]*Tecnológico Nacional de México / Instituto Tecnológico de Mérida, Plan de Ayala, 97118 Mérida, Yucatán, México*

[5]*Tecnológico Nacional de México / Instituto Tecnológico de Tuxtepec, Av. Dr. Víctor Bravo Ahuja No. 561. Col. Predio el Paraíso, 68350 Tuxtepec, Oaxaca, México*

[6]*Universidad del Papaloapan Campus Loma Bonita, DES Ciencias Agropecuarias, Av. Ferrocarril S/N, Cd. Universitaria, 68400 Loma Bonita, Oaxaca, México*

[7]*Colegio de Postgraduados Campus Veracruz, Km. 88.5 Carretera Xalapa-Veracruz, 91690 Veracruz, México*

Article history

Received: 12 October 2019
Received in revised form: 12 August 2020
Accepted: 13 November 2020

Keywords

Image analysis,
pore size distribution,
porosity,
scanning electron microscopy,
tortuosity

Abstract

The objective of the present work was to determine the influence of feeding type and artisanal process on microstructural and physicochemical parameters of goat cheeses. The cheeses were made with goat's milk from goats which were fed with different forages: (1) reed (*Cissu verticillata*) and King grass (*Saccharum sinense*), (2) mulberry (*Morus alba*) leaves and orange (*Citrus sinensis*) peels, (3) alfalfa (*Medicago sativa*) and corn (*Zea mays*) stover, and (4) bellota (*Quercus ilex*) and Kikuyu grass (*Pennisetum clandestinum*). Fresh and ripened artisanal cheeses were analysed by scanning electron microscopy and image analysis. Results showed that goat's milk of goats fed with mulberry leaves and orange peels generated larger conglomerates of fat in both types of cheeses, while the microstructure of the rest of the cheeses presented protein networks. A low pH and moisture content contributed to the formation of lactose crystals which ended in a compact microstructure, propitiating, reduction of the number of pores, porosity, and increase in the breakability of ripened cheeses. Pores of elongated shapes with irregular edges characterised the microstructure of both kinds of cheeses. Through discriminant analysis, it was found that the effect of the type of cheese and type of goat feeding influenced the microstructural and physicochemical parameters such as pore number, porosity, pore size, pore perimeter, roundness, FF, AR, SOL, tortuosity, INP-DI, PAZ, fat, moisture, and pH.

Introduction

Goat cheese is an excellent source of nutrients such as proteins, lipids, vitamins, and minerals, as well as sensory qualities such as appearance, texture, odour, and flavour (Moreno-Rojas *et al.,* 2010). Chemical compositions and physical characteristics can be affected by several factors like genotype, seasonality, animal breed, lactation stage, feeding type, and cheese-making process. Among the factors with greater variability inside production systems, we find that the type of goat feeding affects the chemical quality of cheeses (Almanera *et al.,* 2007). In Mexico, artisanal cheese production ranks third (18.5%) in Gross Domestic Product (GDP) of dairy products in the food industry, and 0.6% of GDP as a whole (INEGI, 2007). Cheeses produced in the goat production systems exhibit duality since they are a form of sustenance for the producers, and represent the place from where they are made (Silva *et al.,* 2015; Ramírez-Rivera *et al.,* 2016). The sensory characteristics of artisanal cheeses are of great importance in order to classify them according to their origin and processing, and to differentiate them from industrial and adulterated cheeses (Ramírez-Rivera *et al.,* 2018). However, one problem commonly found in artisanal production

*Corresponding author.
Email: erasmo_hl@hotmail.com

DOI: https://doi.org/10.47836/ifrj.28.3.02

systems is the lack of control over the critical factors involved in cheese production. This lack of control influences the sensory differences of cheeses even for those of the same category and same production location (Karami *et al.,* 2009; Rovira *et al.,* 2011; 2013).

Microstructure of cheeses has an important role in the sensory aspects (Silva *et al.,* 2015). Frequently used forages for feeding the goats in the Mexican production systems are alfalfa (*Medicago sativa*), reed (*Cissu verticillata*), bellota (*Quercus ilex*), corn (*Zea mays*) stover, King grass (*Saccharum sinense*), Kikuyu grass (*Pennisetum clandestinum*), and mulberry (*Morus alba*) leaves (Ramírez-Rivera *et al.,* 2016; 2018). However, as an alternative to fodder seasonality, producers use by-products of the orange juice industry such as orange (*Citrus sinensis*) peels as a source of food for goats (Ramírez-Rivera *et al.,* 2018). In this regard, Rovira *et al.* (2011) has demonstrated that the industrial processing influences the final microstructure of cheeses. Currently, there is no scientific evidence on the effect of the forages mentioned and the artisanal process in the final microstructure of the goat cheese. The relationship between microstructural and physicochemical parameters would be able to explain the impact of the aforementioned factors on the microstructure of cheeses. From the point of view of the geographical origin of cheeses, the coupling of microscopic and image analysis should also be considered to detect traceability, geographical marker, or type of artisanal cheeses (Moreno-Rojas *et al.,* 2010; Necemer *et al.,* 2016; Ramírez-Rivera *et al.,* 2018). Currently, these tasks have been carried out through proximal chemistry analysis, volatile compounds, mineral elements, instrumental analyses (colour and texture), and sensory analysis for the typing of artisanal cheeses (Moreno-Rojas *et al.,* 2010; Ramírez-Rivera *et al.,* 2018). The visual / qualitative analyses of the cheese microstructure have been performed by the microscopy technique such as Scanning Electronic Microscopy (SEM) on goat cheeses (Karami *et al.,* 2009; Rovira *et al.,* 2011; 2013; Silva *et al.,* 2015; Burgos *et al.,* 2016), sheep cheeses (Fallico *et al.,* 2006), and cow cheeses (Ong *et al.,* 2011). Nevertheless, researchers on the field of image analysis such as Impoco *et al.* (2007) and Silva *et al.* (2015) have generated different algorithms that allow the quantification of microstructural parameters of cheeses such as pore number and shape, granulometry, and the complexity of the microstructure known as tortuosity. These algorithms have been applied specifically to industrial cheeses from Spain and Chile to quantify the changes of the microstructure during its production, and to get better quality control of these products (Leiva *et al.,* 2009; Rovira *et al.,* 2011; 2013; Silva *et al.,* 2015).

Therefore, the objective of the present work was to determine the impact of the feeding type and the artisanal process on the microstructural and physicochemical aspects of two types of goat cheese (fresh and ripened).

Materials and methods

Origin and artisanal process of fresh and ripened cheese

Cheeses from different Goat Production Units (GPUs) were produced. The GPUs were located in the municipalities of Coatepec, Pacho Viejo, Perote, and Tatatila in the state of Veracruz, Mexico. These municipalities are characterised for being a producing area for artisanal goat cheeses. The climatic characteristics of these municipalities, without being considered as study factors, were as follows: warm-humid climate; temperature (12 - 20°C), precipitation (490 - 1,800 mm), and altitude (1,200 - 2,400 m above sea level) (Ramírez-Rivera *et al.,* 2018). The cheeses were made with milk from the Alpine and Saanen goat breeds.

The type of goat feeding (GF) and its content in Coatepec was 40% bejuco (*Cissu verticillate*; protein: 5.36 and fat: 1.92) and 60% King grass (*Saccharum sinense*; protein: 6.85 and fat: 6.39). The GF in Pacho Viejo was 75% mulberry leaves (*Morus alba*; protein: 18.1 and fat: 2.1) and 25% orange peels (*Citrus sinensis*; protein: 6.10 and fat: 3.40). The GF in Perote was 70% alfalfa (*Medicago sativa*; protein: 6.00 and fat: 1.00) and 30% corn stover (*Zea mays*; protein: 5.40 and fat: 1.10). The GF in Tatatila was 35% bellota (*Quercus ilex*; protein: 2.60 and fat: 4.80) and 65% Kikuyu grass (*Pennisetum clandestinum*; protein: 19.50 and fat: 2.74).

The cheese-making process was uniform in all GPUs through the following stages: (1) the goat's milk was pasteurised (stainless steel equipment, Ordemex Industrial, Mexico) at 63°C for 30 min, and cooled at 37°C, (2) 30 mL of commercial rennet (curdling force 1:10,000 or 110 IMCU/mL; Cuamex Industry, Mexico) per 100 L of milk was added, and 45 min later, the curd was cut and pressed (2 kg force per.1 kg cheese) for 7 h in cylindrical moulds of polyvinyl chloride (PVC; 80 mm diameter and 95 mm height) to obtain samples of 300 g, and (3) the obtained curd was immersed in brine (28% salt) for 7 to 8 h, and stored at 25 ± 2°C for 2 d in order to obtain fresh cheeses. Ripened cheeses were prepared by spray-inoculation of *Penicillium candidum*

(Choozit™ PC-VB of the trademark Danisco, Dupont of Mexico) on the fresh cheeses that were obtained earlier. They were then stored in wooden containers for 7 w at 18 ± 2°C and 80 - 85% RH. Cheese samples were packed in high vacuum, and transported at 4 ± 2°C for analyses (Ramírez-Rivera *et al.,* 2016; 2018).

Micrographs of cheeses by Scanning Electron Microscopy (SEM)

Micrographs of cheese by SEM (Electron Microscopy Science, Washington, DC, USA) were obtained as follows: cuts (1 cm^2) of cheese surface were obtained and fixed according to the conditions indicated by Lobato-Calleros *et al.* (2006). A solution of 2.5% w/v glutaraldehyde in 2% of phosphate buffer (0.2 M, pH 7.2) was used to fix cuts for 6 h. Then, each cut was dehydrated in aqueous ethanol solutions with concentrations of 30, 50, 70, 85, 96, and 100% during 30 min for each concentration. Samples were dried to a critical point by employing a dryer (Tousimis Samdri®-795, Rockville MD, USA) and using CO_2 as a transition means. Subsequently, each cut was given a carbon tape for recovery with gold in a vacuum device (Denton Vacuum, DESK III Moorestown, NJ, USA). The cuts in a high vacuum microscope (JEOL, 6360 LV Akishima, Japan) were observed at 20 KV and 1,000× magnification (10 µm). Two micrographs of 8 bits and 1280 × 960 pixels (19 pixels = 1 µm) for each cheese were obtained.

Image analysis: pre-processing of micrographs

The pre-processing of the micrographs consisted of (i) stage 1: calibration according to its magnification (µm); (ii) stage 2: use of medium, Gaussian, and bandpass filters for the removal of noise in the micrographs; and (iii) stage 3: segmentation of micrographs by Otsu automated threshold method (Impoco *et al.,* 2007). This method identified the threshold value that best discriminated the two phases by minimising the intra-class variance while maximising the inter-class variance. The Otsu threshold method is commonly used for the segmentation of dairy product images (Impoco *et al.,* 2007; Silva *et al.,* 2015).

Quantification of microstructural parameters: global morphology and pore shape

The calculated global morphology parameters were (1) pore number, defined as the free cavity between the bonds of proteins observed on the surface of the sample, (2) % porosity (ε) calculated as the percentage of white area (free space in the protein matrix) with respect to the total image area in the binary image, (3) pore size (µm), (4) pore perimeter (µm), and (5) pore area (µm^2) (Impoco *et al.,* 2007; Rovira *et al.,* 2011; 2013). The pore shape parameters were determined according to the method of Impoco *et al.* (2007) using Eqs. 1 - 4:

$$\text{Form factor } (FF) = \frac{4\pi \cdot A}{p^2} \quad \text{(Eq. 1)}$$

$$\text{Round ness } = \frac{4A}{\pi D_{max}^2} \quad \text{(Eq. 2)}$$

$$\text{Aspect ratio (AR)} = \frac{D_{max}}{D_{min}} \quad \text{(Eq. 3)}$$

$$\text{Solidity } (SOL) = \frac{A}{A_{convex}} \quad \text{(Eq. 4)}$$

Where, A = net area (µm^2), A_{convex} = area of the convex hull (µm^2), *p* = perimeter of the pore (µm), Dm_{in} and D_{max} (µm) = minimum and maximum diameter of pore, respectively. The parameters FF, roundness, and AR (dimensionless units) quantified the departure of a feature from the roundness of the pores, and the SOL (dimensionless units) quantified the consistency of the protein matrix (Leiva *et al.,* 2009; Rovira *et al.,* 2013). Pores equal to five pixels were used for the calculations (Impoco *et al.,* 2007). These determinations were made in triplicate at each micrograph type, and for six repetitions.

Quantification of microstructural parameters: granulometry and tortuosity

The granulometric analysis consisted in the determination of the particle size (PAZ) and inter-particle distance (INP-DI). The results were presented by granulometric curves generated by Eq. 5 as proposed by Silva *et al.* (2015):

$$g(i) = \frac{V(i) - V(i+1)}{V(initial) - V(final)} \quad \text{(Eq. 5)}$$

Where, g(*i*) = percent of gray level variation for the step, and *V*(i) = generated curve by counting the number of pixels after each closing or opening step (four steps per procedure). The granulometric curve (GC) was built after the normalisation of the difference of the initial and final number of pixels [*V* (initial), *V* (final)], respectively. For the comparison of GC for a set of samples, each sample was summarised by computing the geometric mean (m). The following weighted sum (Eq. 6) proposed by Silva *et al.* (2015) was used for m:

$$m = \exp\ \left(\sum_{i=1}^{imax} g(i) * \log(ti)\right) \qquad \text{(Eq. 6)}$$

Where, *ti* = size of the structuring element (4 pixels) in µm, and imax = number of closing/opening steps. The geometric means of the GC corresponded to PAZ (opening procedure) or INP-DI (closing procedure) (Legland *et al.,* 2012). In addition, the value of tortuosity (τ) of the microstructure of each cheese was calculated. The τ is defined as the ratio of the shortest path (avoiding the protein network) between the two opposing borders of the image over the Euclidean distance between the same borders. The minimum value of this parameter is 1.0 (Wu *et al.,* 2006; Silva *et al.,* 2015). In order to assess the variability of the τ measurement, each micrograph was divided into three sub-images, and τ was calculated for each sub-image for six repetitions (Silva *et al.,* 2015). The original micrographs were converted into 3D images to visualise the morphological or granulometric aspects (Karami *et al.,* 2009; Hemmatian *et al.,* 2015).

Computational modules of micrographic analysis

The thresholding procedure using BinariseSEM, and the quantification of global morphology and shape parameters using ComputeStats and PoreAnalysis were performed following the method of Impoco *et al.* (2007). The granulometric parameters and τ were calculated with the modules granulometry and geodesic, respectively (Silva *et al.,* 2015; Legland *et al.,* 2012). The 3-D images were performed using "Interactive 3D surface plot" and "Spectrum LUT" (Hemmatian *et al.,* 2015). All programs were operated in by ImageJ version 1.51e (National Institute of Health, Bethesda, MD, USA).

Physicochemical analysis

The cheese fat content was determined following the method of Gerber-Van Gulik, and pH with a potentiometer (Hanna, HI 98230, Milan, Italy) according to García *et al.* (2012). Protein (method 920.123) and moisture (method 948.12) contents were measured following the procedure of AOAC (2005). All analyses were performed in triplicates.

Statistical analysis

Descriptive analyses, one-way ANOVA (p = 0.05), and Tukey *post-hoc* test were performed to determine significant differences (Rovira *et al.,* 2011). Pearson correlation test (r) was used for evaluating the correlation between the microstructural and physicochemical parameters (Rovira *et al.,* 2011). Lastly, discriminating analysis (DA) stepwise procedure was used. This analysis was performed two times, one for each qualitative variable (type of cheese and type of goat feeding) to determine the impact of these variables on the microstructural and physicochemical parameters. In addition, the following statistical indicators derived from stepwise procedure were interpreted; probability values of Wilk's Lambda test (λ) and the percentage of classification (%) was applied to check the discriminatory capacity of the model generated, according to the microstructural and physicochemical parameters (Herman-Lara *et al.,* 2019). Statistical analysis was performed with the software STATGRAPHIC PLUS® version 5.2 (Statistical Graphics Corp, USA). The DA, Wilk's Lambda test (λ), and percentage (%) of classification technique were performed with the XLSTAT 2017 software (version 2015.6.01; Addinsoft, Paris, France).

Results and discussion

Microstructure and image analyses of fresh cheese

Microstructures of fresh cheeses are shown in Figure 1. The microstructures of Perote (Figure 1C) and Tatatila (Figure 1D) cheeses showed free cavities of different sizes which were generated by the heterogeneous dispersions of the casein particles in the protein network (PN). This may be due to the high protein content present in alfalfa-corn stover and bellota-Kikuyu grass feed, respectively (Ramírez-Rivera *et al.,* 2018). Peláez *et al.* (2004) and Soryal et al. (2004) mentioned that alfalfa and pastures contribute to high protein content in the milk used to make cheese. Fat globules (FG) and short lactose crystals (LC) with pyramidal shape (Figure 1A) characterised Coatepec cheese microstructures. The LC formed in the microstructure of Coatepec cheese was consistent with that reported by Pispone *et al.* (2013) who observed short LC in the microstructure of Riccotta cheese at pH 6. They also mentioned that cheese at pH 6 exhibited LC at wide dimensions. The formation of LC is due to obtaining heterogeneous mass with long and short crystals. The micrographs of Pacho Viejo cheese (Figure 1B) showed the predominance of large conglomerates of fat globules (CFG). The large CFG could be associated to the usage of mulberry leaves and orange peels in the diet of goats which then produced milk with higher fat content (Lacerda de Medeiros *et al.,* 2013). According to Bouattour *et al.* (2008), the use of foods with high content of fatty acids (orange peel) contributes to lipogenesis being more active during lactation. Pressing of cheese could also

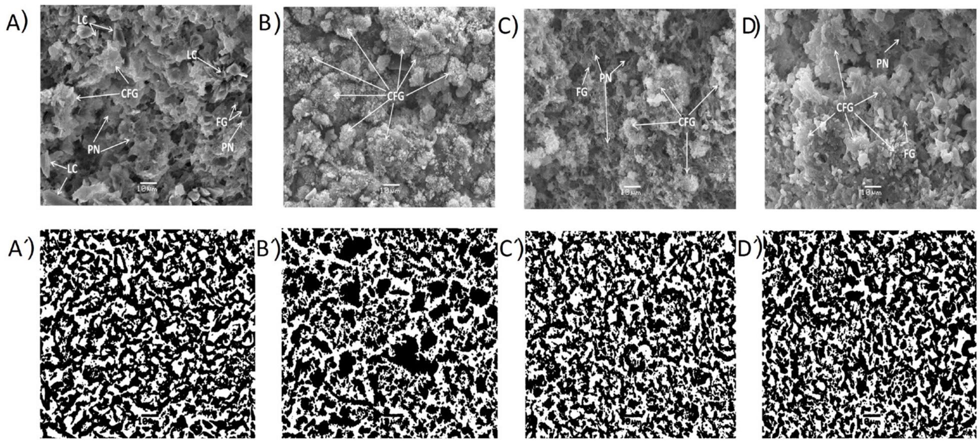

Figure 1. Micrographs of fresh goat cheese (1,000× magnification). (A) Coatepec = reed and King grass; (B) Pacho Viejo = mulberry leaves and orange peels; (C) Perote = alfalfa and corn stover; and (D) Tatatila = bellota and Kikuyu grass, with their corresponding binarised images (A´), (B´), (C´) and (D´), respectively, by Otsu threshold method. Scale bar = 10 µm. CFG = conglomerates of fat globules; LC = lactose crystals; FG = fat globules; and PN = protein network.

contribute in the large CFG due to the breaking of the fat globule membrane, and subsequently, adsorption of proteins occurred (Karami *et al.,* 2009; Rovira *et al.,* 2011). The shape of the fat globules matched with the ones described by Lopez *et al.* (2007) who observed FG and CFG in Emmental cheese. The microstructure of the fresh cheese in the present work showed similarities with the microstructure of Quebrada cheese from Humahuaca, Argentina (Burgos *et al.,* 2016). Tables 1 and 2 show the results of the microstructural and physicochemical parameters of fresh cheese, and the correlations between those parameters. It was observed that Coatepec, Perote, and Tatatila cheeses showed the highest pore number ($p \leq 0.05$). This was confirmed in the binary images (Figures 1A´, 1C´, and 1D´) where larger free cavities are shown (white areas) through the protein network (dark areas). Pacho Viejo cheese showed smaller free spaces in its microstructure (Figures 1B and 1B´). The *ε* of Coatepec, Perote, and Tatatila cheeses (40, 42, and 41%, respectively) were higher than that from Pacho Viejo cheese. The differences in ε could be influenced by pore number ($r_{\text{pore number-}\varepsilon} = 1$), pore size ($r_{\varepsilon\text{-pore size}} = -1.00$), pore perimeter ($r_{\varepsilon\text{-pore perimeter}} = -0.89$), and the pore area ($r_{\text{Pore area-}\varepsilon} = -1$) (Table 2). Thus, Coatepec, Perote, and Tatatila cheeses had smaller pores (14.38, 12.49, and 10.53 µm, respectively) in their microstructures, significantly different from Pacho Viejo cheese (60.11 µm) (Table 1). Pore perimeter was similar among all evaluated cheeses (Table 1). This could be because open spaces were uniformly generated during cheese draining in the aqueous phase, so the pressing contributed to the dispersion of pores in the same way (Boutrou *et al.,* 2002). The generation of significant small areas of pore distribution (5.83, 6.90, and 7.00 µm^2, respectively) in the cheese microstructures from Coatepec, Perote, and Tatatila was defined by the inverse relationship with ε ($r_{\varepsilon\text{-pore area}} = -1.00$) (Table 2). The correlations mentioned agree with the research of Rovira *et al.* (2011). These authors also observed a decrease in the number of pores and ε, and an increase in the pore area of Spanish goat cheeses that are associated with the coalition of curd particles occurring in the cut process. The roundness and FF values were low (Table 1) as compared to those obtained by Leiva *et al.* (2009) who reported values of 0.53 and 0.67, respectively, in Chanco cheese from Chile. According to Impoco *et al.* (2007), low values of roundness and FF indicate that the pores had an elongated shape with irregular edges because of the existence of fat globules aggregates. The pore shape of the fresh cheese was generated by the structural rearrangement caused by the hydrolysis of the caseins (Leiva *et al.,* 2009; Rovira *et al.,* 2013). Other factors such as the strength and the time of the pressing could contribute to the formation of elongated pores (Impoco *et al.,* 2007; Rovira *et al.,* 2011). No significant differences were found in the AR parameter among the evaluated samples of cheese. Pacho Viejo cheese showed an opposite effect to the rest of the samples (Table 1) according to the relationship $r_{\text{AR-SOL}} = -0.95$ (Table 2). The values of AR of the cheese from Coatepec, Perote, and Tatatila are consistent with Leiva *et al.* (2009) who found similar values in cheese samples from

Table 1. Microstructural and physicochemical parameters of fresh and ripened cheeses.

Variable	Fresh cheese				Ripened cheese			
	Coatepec	Pacho Viejo	Perote	Tatatila	Coatepec	Pacho Viejo	Perote	Tatatila
Pore number	532.0 ± 21.21^{a}	49.5 ± 2.12^{b}	573.0 ± 77.78^{a}	542.0 ± 44.5^{a}	362.0 ± 144^{b}	37.0 ± 5^{c}	613.0 ± 87^{a}	547.0 ± 27^{a}
Porosity (%)	40.0 ± 1.00^{a}	23.0 ± 22^{b}	42.0 ± 1.00^{a}	41.0 ± 1.00^{a}	23.0 ± 23^{a}	41.0 ± 3^{a}	42.0 ± 1.00^{a}	41.0 ± 1.00^{a}
Pore size (µm)	14.38 ± 7.28^{b}	60.11 ± 8.43^{a}	12.49 ± 5.08^{b}	10.53 ± 1.42^{b}	11.11 ± 6.94^{b}	62.97 ± 8.71^{a}	16.63 ± 2.23^{b}	9.84 ± 2.73^{b}
Pore perimeter (µm)	21.38 ± 4.05^{a}	24.40 ± 5.56^{a}	20.81 ± 2.60^{a}	18.98 ± 0.12^{a}	18.13 ± 4.56^{a}	81.82 ± 39.77^{b}	23.44 ± 1.50^{a}	18.68 ± 2.11^{a}
Pore area (µm^{2})	5.83 ± 5.83^{b}	128.90 ± 42.37^{a}	6.90 ± 7.68^{b}	7.00 ± 5.47^{b}	3.70 ± 1.65^{a}	5.90 ± 3.34^{b}	5.98 ± 6.42^{a}	6.83 ± 8.65^{a}
Roundness	0.22 ± 0.02^{a}	0.23 ± 0.01^{a}	0.22 ± 0.02^{a}	0.19 ± 0.03^{a}	0.22 ± 0.03^{a}	0.25 ± 0.03^{a}	0.22 ± 0.02^{a}	0.19 ± 0.01^{a}
FF	0.35 ± 0^{a}	0.28 ±0.08^{a}	0.37 ± 0.03^{a}	0.34 ± 0.02^{a}	0.36 ± 0.01^{a}	0.30 ± 0.02^{a}	0.39 ± 0.03^{a}	0.50 ± 0.21^{a}
AR	2.34 ± 0.03^{a}	5.1 ± 3.85^{b}	1.88 ± 0.04^{a}	2.18 ± 0.37^{a}	1.81 ± 0.13^{b}	5.42 ± 0.48^{a}	1.95 ± 0.07^{b}	1.86 ± 0.01^{b}
SOL	0.77 ± 0.01^{a}	0.67 ± 0.08^{a}	0.75 ± 0.01^{a}	0.77 ± 0.03^{a}	0.76 ± 0.02^{a}	0.67 ± 0.05^{a}	0.78 ± 0.04^{a}	0.73 ± 0.03^{a}
τ	1.39 ± 0.75^{a}	1.03 ± 1.14^{a}	1.50 ± 0.13^{a}	1.46 ± 0.11^{a}	1.37 ± 0.13^{a}	1.21 ±0.69^{a}	1.46 ± 0.15^{a}	1.53 ± 0.13^{a}
Protein (%)	19.16 ± 0.36^{d}	21.66 ± 0.16^{c}	22.65 ± 0.13^{b}	25.93 ± 0.16^{a}	25.33 ± 0.35^{a}	15.78 ± 0.37^{c}	18.97 ± 0.15^{b}	15.41 ± 0.2^{c}
Fat (%)	11.86 ± 3.30^{c}	18.73 ± 0.25^{b}	22.07 ± 0.2^{a}	18.67 ± 0.23^{b}	38.87 ± 0.50^{c}	39.57 ± 0.42^{b}	39.10 ± 0.20^{bc}	43.27 ± 0.06^{a}
Moisture (%)	44.40 ± 0.62^{a}	47.04 ± 1.4^{a}	39.9 ± 4^{b}	47.4 ± 0.36^{a}	32.37 ± 0.51^{b}	29.14 ± 0.55^{c}	31.97 ± 0.90^{b}	37.0 ± 0.20^{a}
pH	6.10 ± 0.05^{c}	6.33 ± 0.01^{b}	6.40 ± 0.02^{a}	6.40 ± 0.01^{a}	4.71 ± 0.02^{c}	4.92 ± 0.01^{a}	4.71 ± 0.01^{c}	4.78 ± 0.01^{b}

Values are mean ± standard deviation. Different lowercase superscripts within the same row indicate significant difference (p = 0.05). FF = form factor; AR = aspect ratio; SOL = solidity; τ = Tortuosity. Coatepec = reed and King grass; Pacho Viejo = mulberry leaves and orange peels; Perote = alfalfa and corn stover; and Tatatila = bellota and Kikuyu grass.

Table 2. Correlation values between microstructural and physicochemical parameters of fresh cheeses.

Variables	PONU	ε	POSI	POPE	POAR	Round	FF	AR	SOL	Fat	Protein	Moisture	pH	PAZ	INP-DI	τ
PONU	1.00															
ε	**1.00**	1.00														
POSI	**-1.00**	**-1.00**	1.00													
POPE	-0.89	-0.90	0.92	1.00												
POAR	**-1.00**	**-1.00**	**1.00**	0.89	1.00											
Round	-0.56	-0.58	0.62	0.88	0.57	1.00										
FF	0.95	0.94	-0.92	-0.71	-0.93	-0.30	1.00									
AR	**-1.00**	**-1.00**	**0.99**	0.89	**0.99**	0.56	**-0.95**	1.00								
SOL	**0.97**	**0.96**	**-0.98**	-0.88	**-0.98**	-0.59	0.86	**-0.95**	1.00							
Fat	-0.08	-0.05	0.10	-0.06	0.14	-0.14	0.02	0.02	-0.29	1.00						
Protein	0.18	0.21	-0.23	-0.57	-0.16	-0.82	0.00	-0.21	0.12	0.63	1.00					
Moisture	-0.50	-0.50	0.43	0.14	0.45	-0.29	-0.75	0.53	-0.32	-0.32	0.26	1.00				
pH	-0.11	-0.08	0.11	-0.16	0.17	-0.37	-0.12	0.07	-0.28	0.95	0.82	-0.03	1.00			
PAZ	**1.00**	**1.00**	**-1.00**	-0.89	**-1.00**	-0.57	0.93	**-0.99**	**0.98**	-0.14	0.16	-0.45	-0.16	1.00		
INP-DI	0.73	0.73	-0.78	-0.78	-0.78	-0.66	0.51	-0.70	0.87	-0.58	0.12	0.16	-0.44	**0.78**	1.00	
τ	**0.99**	**0.99**	**-0.98**	-0.91	**-0.98**	-0.60	0.94	**-0.99**	0.93	0.07	0.29	-0.53	0.04	**0.98**	0.66	1.00

Values in bold indicate $p < 0.05$. PONU = pore number; ε = porosity; POSI = pore size; POPE = pore perimeter; POAR = pore area; FF = form factor; AR = aspect ratio; SOL = solidity; PAZ = particle size; INP-DI = inter-particle distance; and τ = tortuosity.

Chanco to Osorno, Chile. These authors reported AR values of 1.82 to 2.20, and they indicated that cheese with values of AR < 5 have a lower probability of fracture due to the high SOL of the protein matrix or network. The low value of SOL and high value of AR found in Pacho Viejo cheese can be attributed to the degradation of casein α_{S1} in the bond phe23 - phe24 (Leiva *et al.,* 2009). The granulometric results are shown in Figure 2, where it was observed that the microstructures of Coatepec, Perote, and Tatatila cheeses had particles of greater size (PAZ = 170 µm), and significantly different from Pacho Viejo cheese (PAZ = 130 µm) (Figure 2A). The INP-DI (Figure 2B) values were 210 µm (Coatepec, Perote, and Tatatila cheeses) and 170 µm (Pacho Viejo cheese). These values showed that the larger the PAZ is, the

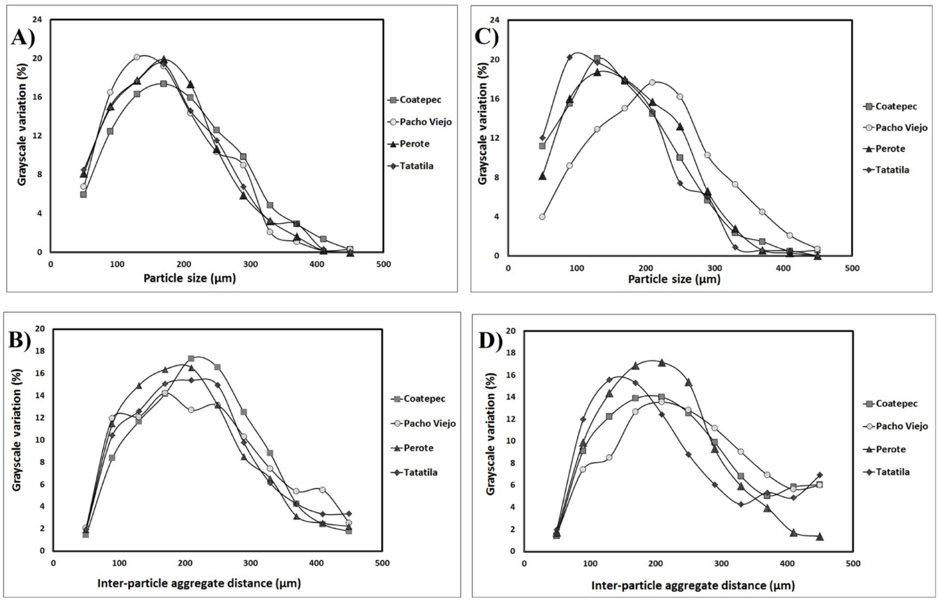

Figure 2. Granulometric curves of fresh [(A) and (B)] and ripened cheeses [(C) and (D)]. (A) and (C) particle size (PAZ) obtained by the opening procedure, and (B) and (D) inter-particle distance (INP-DI) obtained by the closing method. Coatepec = reed and King grass; Pacho Viejo = mulberry leaves and orange peels; Perote = alfalfa and corn stover; and Tatatila = bellota and Kikuyu grass.

greater the inter-distance between the particles appears ($r_{\text{PAZ-INP-DI}}$ = 0.78, Table 2). The low values of granulometry (PAZ) of Pacho Viejo cheese may exist because smaller particles have higher interfaces of an aggregated particle in the aqueous phase (Silva *et al.,* 2015). The values of τ were statistically similar among cheeses (Table 1). The PAZ, number, and size of pore may be related to high values of τ ($r_{\text{PAZ-}\tau}$ = 0.98, $r_{\tau\text{-pores number}}$ = 0.99, $r_{\tau\text{-pore size}}$ = -0.98; Table 2). The values of τ are concordant with Silva *et al.* (2013) who reported a value of τ = 1.5 in cheeses produced with high concentration of proteins. The high values of τ in Perote and Tatatila cheeses were related to high concentration of proteins (22.65 and 25.93%, respectively) and to the obstruction effect of the protein network that increases the long path of diffusion of molecules (Silva *et al.,* 2015). Therefore, the parameters (PAZ, number, and size of the pore) were determinant in cheese texture and in the diffusion of macromolecules in the interior of its microstructure. Silva *et al.* (2013) explained that larger pores allow the mass transfer of smaller molecules.

Microstructure and image analyses of ripened cheese

The micrographs of ripened cheese samples are shown in Figure 3. It was observed that the microstructures of Coatepec (Figure 3A) and Tatatila (Figure 3D) cheeses showed a high prevalence of LC. The pyramidal shape of the LC could be influenced by the low pH (4.71 - 4.92) of ripened cheese in general (Table 1), and its formation may be due to the impediment of the Ca^{2+} and lactate ion movement caused by FG and water-protein bonds (Rajbhandari and Kindsedt, 2008). This result agrees with Pispone *et al.* (2013) who observed LC of pyramidal shape in Riccotta cheese (pH 4). The microstructure of Pacho Viejo ripened cheese (Figure 3B) exhibited LC and mainly large CFG similar to fresh cheese from this municipality. The microstructures of Perote cheese (Figure 3C) were characterised by a more compact PN, with incrustations of FG, CFG, few LC, and some strands. The strands of Perote cheese were generated by the strong interaction between FG and casein micelles (Ong *et al.,* 2011). Zhong *et al.* (2007) indicated that the rearrangements of the structures of ripened cheeses led to the formation of a weak structure formed by strands and crystals. This type of structure could be the reason for the rupture of ripened cheeses. The compaction of the microstructure was related to the loss of moisture (Fallico *et al.,* 2006; Lacerda de Medeiros *et al.,* 2013). In this case, Hemmatian *et al.* (2015) noticed that the use of NaCl generates an increase in the hydrophobic interactions between proteins that contribute to the compacting of protein network. Thus, the method of salting by immersion applied in the production of the cheese in the present work was able to contribute in generating these interactions as

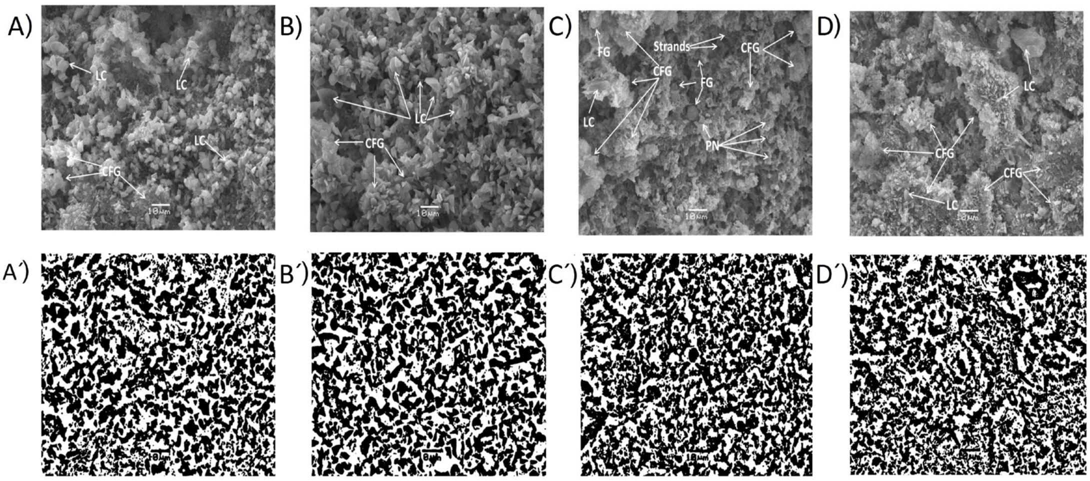

Figure 3. Micrographs of ripened goat cheese (1,000× magnification). (A) Coatepec = reed and King grass; (B) Pacho Viejo = mulberry leaves and orange peels; (C) Perote = alfalfa and corn stover; and (D) Tatatila = bellota and Kikuyu grass, with their corresponding binarised images (A′), (B′), (C′) and (D′), respectively, by Otsu threshold method. Scale bar = 10 µm. CFG = conglomerates of fat globules; LC = lactose crystals; FG = fat globules; and PN = protein network.

compared to other methods of salting, such as surface salting. Tables 1 and 3 show the results of the microstructural and physicochemical parameters of ripened cheeses, and the correlations between those parameters. A reduction was observed in the number of pores (Table 1), where the cheese from Pacho Viejo exhibited the least significant amount; this effect was related to the loss of moisture ($r_{\text{pore number-moisture}}$ = 0.75, Table 3). The reduction in the number of pores among fresh and ripened cheeses from Coatepec and Pacho Viejo could be due to the decrease of free water, which caused a contraction effect in the protein network and obstruction of the diffusion of molecules (Chapeau *et al.,* 2016). While the increase in the pore number of the cheeses from Perote and Tatatila could be due to the high permeability of the protein network caused in the stage of the curd cut (Rovira *et al.,* 2013). The values of *ε* were similar ($p \geq 0.05$) for all cheeses, while the perimeter of the pores and area of the pores were different ($p \leq 0.05$) for all cheeses. These results were supported by the value correlations of $r_{\varepsilon\text{–pore area}}$ = 0.97 (Table 3). Rovira *et al.* (2013) also reported the same trend in goat cheese from Murcia, Spain. In the case of Pacho Viejo cheese, it showed a more open structure because it contained larger pores

Table 3. Correlation values between microstructural and physicochemical parameters of ripened cheeses.

Variable	PONU	ε	POSI	POPE	POAR	Roundness	FF	AR	SOL	Fat	Protein	Moisture	pH	PAZ	INP-DI	τ
PONU	1.00															
ε	-0.04	1.00														
POSI	-0.88	0.39	1.00													
POPE	-0.88	0.41	**1.00**	1.00												
POAR	0.22	**0.97**	0.16	0.18	1.00											
Roundness	-0.76	0.00	0.87	0.84	-0.18	1.00										
FF	0.76	0.29	-0.74	-0.71	0.47	**-0.95**	1.00									
AR	-0.90	0.40	**1.00**	**1.00**	0.17	0.83	-0.70	1.00								
SOL	0.86	-0.49	-0.84	-0.86	-0.25	-0.48	0.36	-0.88	1.00							
Fat	0.48	0.60	-0.41	-0.37	0.69	-0.79	0.92	-0.36	-0.02	1.00						
Protein	-0.41	-0.87	-0.02	-0.03	**-0.96**	0.20	-0.48	-0.01	0.00	-0.61	1.00					
Moisture	0.75	0.35	-0.24	-0.19	0.33	-0.67	0.69	-0.15	-0.33	0.83	-0.14	1.00				
pH	0.75	0.21	-0.38	-0.40	0.42	-0.19	0.30	-0.44	0.68	0.13	-0.65	-0.44	1.00			
PAZ	-0.81	-0.09	0.85	0.83	-0.28	**0.99**	**-0.98**	0.82	-0.50	-0.82	0.32	-0.63	-0.29	1.00		
INP-DI	-0.55	-0.57	0.47	0.44	-0.68	0.82	-0.94	0.42	-0.06	**-1.00**	0.62	-0.79	-0.20	0.86	1.00	
τ	**0.95**	0.09	-0.88	-0.87	0.33	-0.91	0.92	-0.87	0.69	0.71	-0.45	0.36	0.58	-0.95	-0.77	1.00

Values in bold indicate $p < 0.05$. PONU = pore number; ε = porosity; POSI = pore size; POPE = pore perimeter; POAR = pore area; FF = form factor; AR = aspect ratio; SOL = solidity; PAZ = particle size; INP-DI = inter-particle distance; and τ = tortuosity.

Table 4. Average and probability values for each microstructural and physicochemical parameter by qualitative variable (type of cheese and goat feeding).

Variable	Type of cheese			Type of goat feeding				Pr < Lambda
	Fresh	Ripened	Pr < Lambda	Alfalfa and corn stover	Bejuco and King grass	Bellota and Kikuyu grass	Mulberry leaves and orange peels	
Pore number	424.25	389.50	> 0.05	592.75	447.00	544.75	43.00	< 0.0001
Porosity (%)	0.37	0.36	> 0.05	0.39	0.32	0.42	0.32	< 0.0001
Pore size (µm)	24.38	25.14	> 0.05	14.56	12.75	10.18	61.54	< 0.0001
Pore perimeter (µm)	21.39	35.52	< 0.0001	22.13	19.75	18.83	53.11	0.0001
Pore area (µm^2)	37.31	5.60	> 0.05	6.44	5.08	6.91	67.40	> 0.05
Roundness	0.22	0.22	> 0.05	0.22	0.22	0.19	0.24	< 0.0001
FF	0.33	0.39	> 0.05	0.38	0.36	0.42	0.29	0.0001
AR	2.89	2.76	> 0.05	1.91	2.07	2.02	5.30	< 0.0001
SOL	0.74	0.73	< 0.0001	0.77	0.76	0.75	0.67	< 0.0001
Tortuosity	1.34	1.40	> 0.05	1.48	1.38	1.50	1.13	< 0.0001
INP-DI (µm)	204.75	199.88	< 0.0001	199.75	230.00	179.75	199.75	0.0001
PAZ (µm)	159.50	149.75	< 0.0001	159.75	159.75	129.50	169.50	0.002
Fat (%)	17.44	40.09	< 0.0001	30.63	24.38	30.93	29.13	> 0.05
Protein (%)	22.40	18.91	> 0.05	20.81	22.43	20.67	18.72	> 0.05
Moisture (%)	44.21	32.82	< 0.0001	35.66	38.30	42.26	37.85	0.001
pH	6.31	4.78	< 0.0001	5.54	5.44	5.58	5.63	> 0.05

(62.97 µm) as compared to the rest of the evaluated samples of cheese (Table 1). The increase in pore size of Pacho Viejo cheese was due to the microbial fermentation process that additionally increased the surface roughness of the cheese samples (Hemmatian *et al.,* 2015). The open structures of the goat cheese are related to the hydration of the protein matrix or network caused by the thermal treatment of milk (Burgos *et al.,* 2016). The values of the parameters roundness, FF, and SOL were similar ($p \geq 0.05$) among the cheese samples (Table 1). The value of AR (5.42) of Pacho Viejo cheese was significantly higher, and therefore the SOL of the protein matrix was smaller ($r_{AR\text{-}SOL}$ = -0.88, Table 3). The aforementioned could contribute to the firmness of this variety of cheeses (Mistry *et al.,* 2006). The roundness values obtained in the present work are consistent with those reported by El-Zeini (2006) in goat cheese (0.33). The values of FF (0.30 to 0.50) of ripened cheeses presented in Table 1 are lower than those reported by Leiva *et al.* (2009) who obtained values of 0.75 of FF in Chanco cheese with 21 d of maturation. On the other hand, Impoco *et al.* (2007) mentioned that the lower the values of FF means that the pores have an elongated shape. The values AR and SOL of the Coatepec, Perote, and Tatatila cheeses indicated that these had a greater resistance to deformation (Leiva *et al.,* 2009) as compared to Pacho Viejo cheese that showed an opposite trend. According to Zhong *et al.* (2007), the rearrangements of the structures of ripened cheeses lead to the formation of a weak structure formed by strands and crystals. This type of structure may be another reason why ripened cheeses have greater breakability than fresh cheeses. Figure 2C shows that the values of PAZ were higher ($p \leq 0.05$) in the Pacho Viejo cheese (PAZ = 210 µm) in comparison to the other cheeses (PAZ between 90 - 130 µm); this parameter was related to pore perimeter ($r_{PAZ\text{-pore perimeter}}$ = 0.83) and pore size ($r_{PAZ\text{-pore size}}$ = 0.85) (Table 3). Figure 2D shows that Tatatila cheese had the smallest value of INP-DI (130 µm) in relation to the other cheeses (INP-DI = 210 µm), where the moisture and fat content correlated with the INP-DI ($r_{INP\text{-}DI\text{-moisture}}$ = -0.79 and $r_{INP\text{-}DI\text{-fat}}$ = -1.00, Table 3). The high values of PAZ (210 µm) indicated pores of large perimeters and sizes, which may contain trapped fat globules. The smallest values of INP-DI (130 µm) of cheeses could be generated by high moisture and fat contents. The τ did not show significant difference ($p \geq 0.05$) for all cheeses. This was also observed by Silva *et al.* (2015) in cheeses made with similar casein concentrations. Nevertheless, the cheeses from Perote and Tatatila showed the highest values of τ (1.46 and 1.53), respectively. This could be due to the increase in the size of the aggregates which generate longer paths between the given points (Silva *et al.,* 2013; 2015).

Table 4 shows the mean and probability values of the Wilk's Lambda test for each of the microstructural and physicochemical parameters according to the cheese type and goat feeding type. It was observed that the variables such as pore perimeter, SOL, INP-DI, PAZ, fat, moisture, and pH were significantly discriminated ($p \leq 0.05$) between fresh and ripened cheeses. However, variables such as pore number, porosity, pore size, pore perimeter, roundness, FF, AR, SOL, tortuosity, INP-DI, PAZ, and moisture significantly discriminated ($p \leq 0.05$) the cheese type according to the type of goat's feed. The aforementioned was supported by the DA in Figure 4, in which it is shown that fresh cheeses had a higher content of SOL, INP-DI, PAZ, moisture, and pH; and ripened cheeses had a higher content of fat and pore perimeter (Figure 4A). In the case of goats fed with mulberry leaves and orange peels, it was observed that the cheeses produced had higher content of pore perimeter, pore size, roundness, PAZ, and AR, while the cheeses made from goats fed with Kikuyu grass, bejuco and King grass, and alfalfa and corn stover presented similar characteristics of pore number, porosity, tortuosity, FF, SOL, INP-DI, and moisture (Figure 4B). Finally, the percentages of classification of the cheese samples were 100% in function to the microstructural and physicochemical parameters, and according to the type of cheese and type of goat feeding.

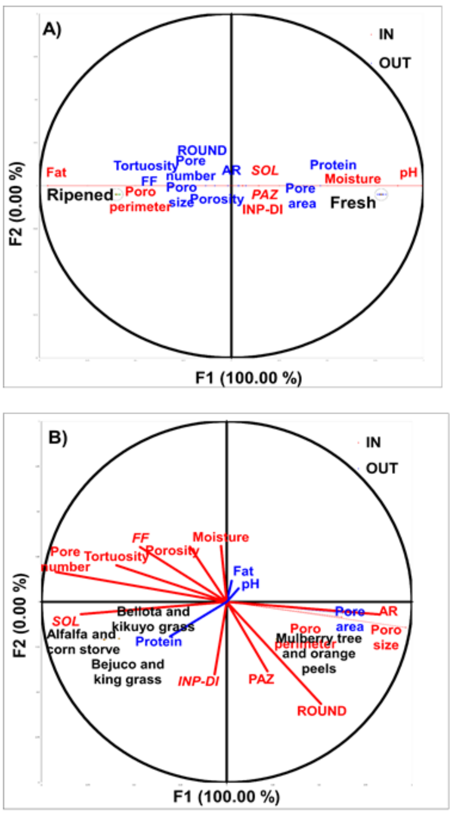

Figure 4. Multivariate representation via Discriminant Analysis (DA) according to (A) type of cheese (fresh or ripened), and (B) type of goat feeding. IN = indicates that the variable helps to differentiate, and OUT = indicates that the variable does not help to differentiate.

Conclusions

The goat's milk from goats which were fed with mulberry leaves and orange peels generated larger conglomerates of fat in both types of cheese microstructures, while the rest of the cheeses were characterised by having protein networks. The low pH and moisture content contributed to the formation of lactose crystals of different dimensions, and in the compaction of the microstructure, which contributed to the decrease in the number of pores, porosity, and increase in breakability of ripened cheeses. The artisanal process of cheese (mainly the cutting of the curd, pressing, and salting) influenced the parameters such as pore number, pore size, pore area, pore particle size, and the generation of cheeses with pores of elongated shapes with irregular edges. Likewise, the fat content contributed to complex microstructure or carried greater tortuosity in the cheeses evaluated in the present work. The DA results showed that the microstructural and physicochemical parameters such as SOL, INP-DI, PAZ, fat, moisture, and pH allowed us to observe differences between fresh and ripened cheeses. However, the type of goat feeding was influenced by 12 out of 16 microstructural and physicochemical parameters evaluated namely pore number, porosity, pore size, pore perimeter, roundness, FF, AR, SOL, tortuosity, INP-DI, PAZ, and moisture. The results of the present work can be a guideline for the analysis of the complexity of the microstructure and its relationship with the release of aromas using chromatography and sense-metric techniques such as Temporal Dominance Sensations. Additionally, these results also pave a way to perform the microstructural-typing of artisanal cheeses, which can be complemented with different analytical and instrumental results to give more information about artisanal cheeses of interest.

Acknowledgement

The authors are grateful to the Scientific Research Centre of Yucatán (Centro de Investigación Científica de Yucatán; CICY) for the assistance in obtaining the micrographs of artisanal cheeses.

References

Almanera, F. J., Álvarez, S., Darias, J., Rodríguez, E., Díaz, C. and Fresno, M. 2007. Effect of the ripening in the mineral composition of the cheeses made with Majorera goat's milk. Archivos de Zootecnia 56: 667-671.

Association of Official Analytical Chemists (AOAC). 2005. Official methods of analysis of

AOAC International. 15th ed. United States: AOAC.

Bouattour, M. A., Casals, R., Albanell, E., Such, X. and Caja, G., 2008. Feeding soybean oil to dairy goats increases conjugated linoleic acid in milk. Journal of Dairy Science 91: 2399-2407.

Boutrou, R., Famelart, M. H., Gaucheron, F., Le Graet, Y., Gassi, J. Y., Piot, M. and Leonil, J. 2002. Structure development in a soft cheese curd model during manufacture in relation to its biochemical characteristics. Journal of Dairy Research 69: 605-618.

Burgos, L., Pece, N. and Maldonado, S. 2016. Proteolysis, texture and microstructure of goat cheese. International Journal of Engineering and Applied Sciences 3: 2394-3661.

Chapeau, A. L., Silva, J. V. C., Schuck, P., Thierry, A. and Floury, J. 2016. The influence of cheese composition and microstructure on the diffusion of macromolecules: a study using Fluorescence Recovery After Photobleaching (FRAP). Food Chemistry 192: 660-667.

El-Zeini, H. M. 2006. Microstructure rheological and geometrical properties of fat globules of milk from different animal species. Polish Journal of Food and Nutrition Sciences 56: 147-154.

Fallico, V., Tuminello, T., Pediliggieri, C., Horne, J., Carpino, S. and Licitra, G. 2006. Proteolysis and microstructure of Piacentinu Ennese cheese made using different farm technologies. Journal Dairy Research 89: 37-48.

García, V., Rovira, S., Teruel, R., Boutoial, K., Rodríguez, J., Roa, I. and López, M. B. 2012. Effect of vegetable coagulant, microbial coagulant and calf rennet on physicochemical, proteolysis, sensory and texture profiles of fresh goat cheese. Dairy Science and Technology 92: 691-707.

Hemmatian, M., Aminifar, M. and Attar, F. 2015. Characterization of Poosti cheese, a traditional raw sheep cheese during ripening: physicochemical, microbial and micro-structural aspects. Nutrition and Food Sciences Research 2: 39-48.

Herman-Lara, E., Bolívar-Moreno, D., Toledo-López, V. M., Cuevas-Glory, L., Lope-Navarrete, M., Barrón-Zambrano, J. A., ... and Herman-Lara, E. J. 2019. Minerals multi-element analysis and geographical origin of artisanal goat cheeses. Food Science and Technology 39(2): 517-525.

Impoco, G., Carrato, S., Caccamo, M., Tuminello, L. and Licitra, G. 2007. Quantitative analysis of cheese microstructure using SEM imagery. In Proceedings of the Società Italiana di Matematica Applicata e Industriale (SIMAI) Congress, p. 1-10. Rome, Italy.

Instituto Nacional de Estadística y Geografía (INEGI). Agricultural, livestock and forestry census 2007. Retrieved on August 20, 2019, from INEGI Website: https://www.inegi.org.mx-/programas/cagf/2007/

Karami, M., Ehsani, M. R., Mousavi, S. M., Rezaei, K. and Sfari, M. 2009. Microstructural properties of fat during the accelerated ripening of ultra-filtered-Feta cheese. Food Chemistry 113: 424-434.

Lacerda de Medeiros, E. J. R., Egypto-Queiroga, R. C. R., Nunes de Medeiros, A., Delmondes-Bomfim, M. A., Malveria-Batista, A. S., Dos Santos-Félex, S. S. and Madruga, M. S. 2013. Sensory profile and physicochemical parameters of cheese from dairy goats fed vegetable oils in the semiarid region of Brazil. Small Ruminant Research 113: 211-218.

Legland, D., Devaux, M. F., Bouchet, B., Guillon, F. and Lahaye, M. 2012. Cartography of cell morphology in tomato pericarp at the fruit scale. Journal of Microscopy 247: 78-93.

Leiva, J. I., Magariños, H. E., Romero, A. F. and Figueroa, H. 2009. Structural characterization by image analysis of Chanco cheese made in the Province of Osorno. Agro Sur 37: 26-33.

Lobato-Calleros, C., Ramos-Solís, L., Santos-Moreno, A. and Rodríguez-Huezo, M. E. 2006. Microstructure and texture of panel type cheese-like products: use of low methoxyl pectin and canola oil as milk-fat substitutes. Revista Mexicana de Ingeniería Química 5: 71-79.

Lopez, C., Camier, B. and Gassi, G. Y. 2007. Development of milk fat microstructure during the manufacture and ripening of Emmental cheese observed by confocal laser scanning microscopy. International Dairy Journal 17: 235-247.

Mistry, V., Hassan, A. N. and Acharya, M. R. 2006. Microstructure of pasteurized process cheese manufactured from vacuum condensed and ultra-filtered milk. Lait 86: 453-459.

Moreno-Rojas, R., Sánchez-Segarra, P. J., Cámara-Martos, F. and Amaro-López, M. 2010. Multivariate analysis techniques as tools for categorization of Southern Spanish cheeses: nutritional composition and mineral content. European Food Research and Technology 231: 841-851.

Necemer, M., Potocnik, D. and Ogrinic, N. 2016. Discrimination between Slovenian cow, goat and sheep milk and cheese according to geographical origin using a combination of elemental content and stable isotope data. Journal of Food Composition and Analysis 52: 16-23.

Ong, L., Dagastine, R. R., Kentish, S. E. and Gras, S. L. 2011. Microstructure of milk gel and cheese curd observed using cryo-scanning electron microscopy and confocal microscopy. LWT - Food Science and Technology 44: 1291-1302.

Peláez, P., Fresno, M., Rodríguez, E., Darías, J. and Díaz, C. 2004. Chemometrics studies of fresh and semi-hard goats cheese produced in Tenerife (Canary Islands). Food Chemistry 88: 361-366.

Pispone, A., Pajumägi, S., Mootse, H., Karus, A. and Poikalainen, V. 2013. The lactose from Riccotta cheese whey: the effect of pH and concentration on size and morphology of lactose crystals. Dairy Science and Technology 93: 477-486.

Rajbhandari, P. and Kindstedt, P. S. 2008. Characterization of calcium lactate crystals on Cheddar cheese by image analysis. Journal of Dairy Science 91: 2190-2195.

Ramírez-Rivera, E. J., Juárez-Barrientos, J. M., Rodríguez-Miranda, J., Díaz-Rivera, P., Ramón-Canul, L. G., Herrera-Corredor, J. A., ... and Herman-Lara, E. 2016. Typification of a goat fresh cheese of Mexico by path models. Turkish Journal of Veterinary and Animal Sciences 41: 213-220.

Ramírez-Rivera, E. J., Ramón-Canul, L. G., Torres-Hernández, G., Herrera-Corredor, J. A., Juárez-Barrientos, J. M., Rodríguez-Miranda, J., ... and Díaz-Rivera, P. 2018. Typing aged goat cheese produced in the mountainous central region of the state of Veracruz, Mexico. Agrociencia 52: 15-34.

Rovira, S., Belen-López, M., Ferrandini, E. and Laencina, J. 2011. *Hot topic*: microstructure quantification by scanning electron microscopy and image analysis of goat cheese curd. Journal of Dairy Research 94: 1091-1097.

Rovira, S., García, V., Laencina, J. and Belen-López, M. 2013. Microstructure of industrially manufactured goat cheese Queso de Murcia al Vino during syneresis. International Journal of Dairy Technology 66: 382-389.

Silva, J. V. C., Leglnad, D., Cauty, C., Kolotuev, I. and Floury, J. 2015. Characterization of the microstructure of dairy systems using automated image analysis. Food Hydrocolloids 44: 360-371.

Silva, J. V. C., Peixoto, P. D. S., Lortal, S. and Floury, J. 2013. Transport phenomena in a model cheese: the influence of the charge and shape of solutes on diffusion. Journal of Dairy Science 96: 6186-6198.

Soryal, K., Zeng, S., Min, B., Hart, S. and Beyene, F. 2004. Effect of feeding system on composition of goat milk and yield of Domiati cheese. Small Ruminant Research 54: 121-129.

Wu, Y. S., Van-Vliet, L. J., Frijlink, H. W. and Van der Voort, M. K. 2006. The determination of relative path length as a measure for tortuosity in compacts using image analysis. European Journal of Pharmacology 2: 433-440.

Zhong, Q., Daubert, C. R. and Orilin, D. V. 2007. Physicochemical variables affecting the rheology and microstructure of rennet casein gels. Journal of Agricultural and Food Chemistry 55: 2688-2697.